THE INTERNATIONAL CONFERENCE ON THE 120TH ANNIVERSARY OF THE BULNAY EARTHQUAKE: ADVANCES IN ASTRONOMY AND GEOPHYSICS

# Aftershock sequences of the Busingol earthquakes of 1974, 1976 and 1991

Kakourova A. A., Dem'yanovich V. M., Djurik V. I., Bryzhak E. V., Klyuchevskaya A. A.
Institute of the Earth's Crust SB RAS, Irkutsk, Russia, anna2015@crust.irk.ru

## Introduction

One of the main tasks of statistical research of seismicity is to study the regularities of spatiotemporal and energy distribution of shock groups and clustered earthquakes. The study of aftershock and swarm sequences of shocks of the Baikal Rift System (BRS) is devoted to the works, which consider the spatial, temporal and energy distributions of events, determine the dynamic parameters of sources and characteristics of the focal environment. It was established that grouping is one of the main properties of BRS earthquake assemblies, and the high saturation of the lithosphere with event groups predetermines strong spatiotemporal variability and the dependence of estimates of the parameters of regional seismicity and the seismic process on clustered shocks, which has not yet been taken into account. This determines the relevance of identifying and classifying groups and clustered earthquakes of the BRS for the purpose of subsequent study of the spatiotemporal and energy distribution, analysis and accounting for the degree of their influence on regional seismicity, creation and testing of models for describing the components of the seismic field and process.

In this paper, we present a statistical study of the spatiotemporal structure of aftershock sequences that occurred on the southwestern flank of the BRZ in the Belino-Busingolsky fault zone after two moderate tremors in 1974 ($K_p$=14), 1976 ($K_p$=14) and a strong earthquake in 1991 ($K_p$=16.2). By studying the structure of aftershock sequences, we mean identifying stable patterns in the distribution of tremors in space and time, ensuring the identity and preservation of the main properties on different spatiotemporal scales.Primary materials are taken from the “Catalog of earthquakes in the Baikal region”, which presents basic information on the seismicity of the Baikal region [http://seis-bykl.ru/].

## Study area and research methods

The influence of aftershock sequences on seismicity and the seismic process depends not only on the number and energy of repeated shocks, but also on the “background” level of seismicity of the studied area. The lower the level of the lithosphere hierarchy, the greater the relative jump in the density of epicenters and the velocity of the flow of seismic events that occurs as a result of an aftershock series, and the more the parameters and characteristics of seismicity of the studied area change. These features of the local spatio-temporal and energy implementation of seismicity were used to identify groups of shocks and clustered earthquakes in the lithosphere of the Baikal region.

In order to maintain the methodological homogeneity of identifying clustered earthquakes from the “Catalogue of Pribaikalye Earthquakes”, we use a combination of the sliding window method and the cluster method – simple methods of identifying events based on their spatio-temporal proximity. The main shock and clustered events are determined within a spatio-temporal window, provided that the number of events within the window exceeds the number of “background” earthquakes of a representative energy class. The main feature for identifying clustered seismicity is a significant change in the gradient of the event flow velocity in the window relative to the background, which makes it possible to establish the start time and estimate the end time of the sequence.

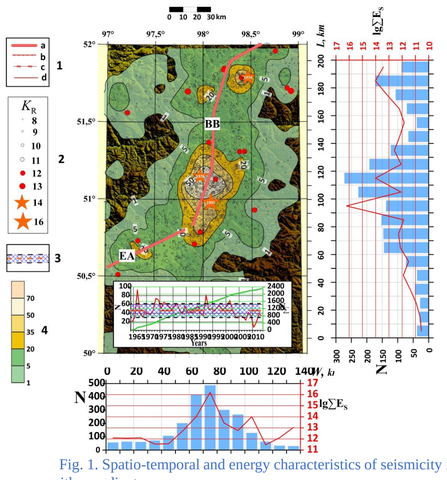


Fig. 1. Spatio-temporal and energy characteristics of seismicity in the area with coordinates

Inset A shows graphs of variations in annual lgN and summed over years ΣN numbers of earthquakes.

1 – faults (a – main [Dem’yanovich et al., 2008b]; additional: b – normal faults, c – strike-slip faults, d – unspecified type [Bachmanov et al., 2017]), 2 – boundaries of rectangular aftershock areas (marked with the year of the beginning of the series), 3 – epicenters of earthquakes with energy class $K_p \geq 8$ (1964–2013), 4 – scale of isolines of epicenter density in 10 × 10 km² areas.

The aftershock sequences of the Busiyngol earthquakes occurred within the area with coordinates φ = 50–52 º N, λ = 97–99 E. The seismicity of this area is presented in fig. 1 as a map of earthquake epicenters with $K_p \geq 8$ for 1964-2013 and isolines of epicenter density n in elementary areas of 10 × 10 km². The dimensions of the selected elementary area correspond to the average error in determining the coordinates of the BRS shock epicenters, and the time interval includes the periods of predominantly “background” seismicity in 1964-1973, the aftershock series of 1974 and 1976, and the sequence of 1991 (fig. 1A). The map shows that the isoline of increased epicenter density $n \geq 5$ is stretched along the BB fault zone and ends in the northeastern segment of the Erzin-Agordak (EA) fault approaching from the southwest. Two areas of high epicenter density are clearly visible, created in the north by the aftershocks of 1974 (maximum density $n$ = 80) and a set of aftershocks of 1976 and 1991 in the central part of the map ($n$ = 822). The main earthquakes of 1976 and 1991 occurred quite close to each other, the rectangular platforms of aftershocks are combined, and the epicentral fields of aftershocks are superimposed and create one common area of high epicenter density on the map. Three rectangular areas show the territories within which the aftershocks of the Busingol earthquakes of 1974, 1976 and 1991 were localized: the aftershock sequence of 1991 occupies the largest area ($S \approx 7370$ km²), a slightly smaller area is occupied by the series of aftershocks of 1976 ($S \approx 5860$ km²) and the minimum is 1974 ($S \approx 2320$ km²). Inside the aftershock areas, the high-density isolines of epicenters $n > 20$ have an elongated oval shape according to the BB fault zone; the ovals fit completely into the areas, and the epicenters of the main earthquakes are located in their central part.

The aftershock series caused by the earthquake of 29.11.1974 ended after the main shock of 01.04.1976. It can be assumed that the main earthquake of 1976 caused aftershock activity until 1983, when the condition $N < N_{fon}$ was met for the first time. After the main earthquake of 1991, aftershock activity for the first time became lower than Nfon in 2003, but then activation occurred in 2004-2006, when $> N_{fon}$.

## Results

The results of identifying the aftershock sequences are shown in fig. 2. The aftershock series of 1974 occurred in the vicinity of the Belinskaya Depression in the north of the BB fault in the area φ = 51.48–51.97 º N, λ = 98.18–98.80 º E. fig. 2A shows the spatio-temporal and energy distributions of 78 aftershocks with $K_p \geq 8$, recorded from November 29, 1974 to April 1, 1976. The epicenter of the main earthquake is located almost in the center of the area, the epicenters of the aftershocks are scattered around the main event, and the shock density isolines have the shape of nested ovals, the long axes of which are shifted to the east of the BB fault and extended in the northeastern direction. The ovals are completely inscribed in the rectangular area of aftershocks, but the n=1 isoline slightly extends beyond the 95% level of the shock dispersion ellipse. The center of the dispersion ellipse and the epicenter of the main earthquake are close and are located at the density maximum $n \geq 20$, i.e. most of the aftershocks occurred in the central part of the focal zone of the main earthquake, but at the 99.9% level the dispersion ellipse slightly extends beyond the rectangular area. The maxima of the seismic energy $lg\ \Sigma E_S$ of the aftershocks correspond to the maxima of the numbers of aftershocks n, realized in the 10 km wide strips intersecting the map in longitude (fig. 2A, below the map) and latitude (fig. 1, to the right of the map). The graphs of variations in annual $N$ and a histogram of the numbers of earthquakes summed over years $\Sigma N$ for 1964-1976 are presented above the map. Note that the increase in N in 1968 was due to a small swarm (φ = 51.65–51.80 º N, λ = 98.35–98.45 º E, 6 events with $K_p$=8–9 within 9 hours). In the interval 1964-1973, the annual values of $N$ are low. The energy class of the three strongest aftershocks is $K_p$ = 11, and the difference between the classes of the main earthquake and the maximum aftershock is $\Delta K_p$ = 3 (the difference in magnitudes $\Delta M_{LH} \approx 1.5$). The main earthquake was preceded by 8 foreshocks with $K_p$ = 8 (7 events), 11 of which occurred in the interval 12 days – 6 hours before it.

The aftershock sequence of 1976 was realized in the vicinity of the Busingol depression in the southern sector of the BB fault. Figure 2B shows the spatio-temporal and energy distributions of 571 aftershocks with $K_p \geq 8$, recorded in the area φ = 50.70–51.44 º N, λ = 97.40–98.42 º E from 01.04.1976 to 31.12.1982. It is evident that the aftershocks were grouped near the main earthquake, but the density isoline $n$ = 1 occupies the entire area, which indicates an increased dispersion of shocks over the territory. The density isolines $n \geq 5$ have the shape of nested ovals slightly shifted to the west and elongated along the BB fault zone, which completely fit into the rectangular aftershock area, but the shape of the isolines is less isometric than in Fig. 6A, B. At the 95% level, the shock dispersion ellipse fits into the area, but at the 99% and 99.9% levels, the ellipses extend significantly beyond its limits. The close location of the dispersion ellipse center and the epicenter of the main shock indicates that the main number of aftershocks were realized in the focal zone of the main shock. The maxima of the seismic energy $lg\ \Sigma E_S$ of the aftershocks correspond to the maxima of the numbers of aftershocks n, realized in the 10-km-wide strips intersecting the map in longitude (fig. 2B, below the map) and latitude (Fig. 6B, to the right of the map). Above the map are graphs of variations in annual $N$ and a histogram of the summed-up annual $\Sigma N$ numbers of earthquakes for 1964-1984.

The aftershock sequence of 1991 was realized in the vicinity of the Busingol depression in the south of the BB fault. Figure 2C shows the spatio-temporal and energy distributions of 4019 aftershocks with $K_p \geq 8$, recorded in the area φ = 50.60–51.55 º N, λ = 97.60–98.60 º E from 27.12.1991 to 31.12. 2009. It is evident that the aftershocks were grouped near the main earthquake. The density isolines of the epicenters fit completely into the area and have an isometric shape of nested ovals elongated along the BB fault zone. The ovals fit completely into the rectangular aftershock area, as do all three levels of the shock dispersion ellipse. The close location of the dispersion ellipse center and the epicenter of the main earthquake indicates that the overwhelming majority of aftershocks were realized in the central part of the focal zone of the main earthquake. The maxima of the seismic energy $lg\ \Sigma E_S$ of the aftershocks are in good agreement with the maxima of the numbers of aftershocks n realized in the 10 km wide strips intersecting the map in longitude (fig. 2B, below the map) and latitude (fig. 2C, to the right of the map). Above the map are graphs of variations in annual $N$ and a histogram of the numbers of earthquakes summed over years $\Sigma N$ for 1983-2009. Comparison of the level of “background” seismicity $N_{fon}$ with the aftershock flow rate shows that formally the sequence lasted until the end of 2001, when the aftershock activity became lower than $N_{fon}$ for the first time. Then the graph shows alternation of weak (2002-2003) and increased (2004-2006), weak (2007) and increased (2008) aftershock activity. The first aftershock had class $K_p$ = 10.2 and was registered 17 min 27.9 sec after the main shock, the energy class of the strongest aftershock was $K_p$ =13.9 (27.04.2005; 07-36-09.1), and D$K_p$ = 2.3 (D$M_{LH} \approx$ 1.1).

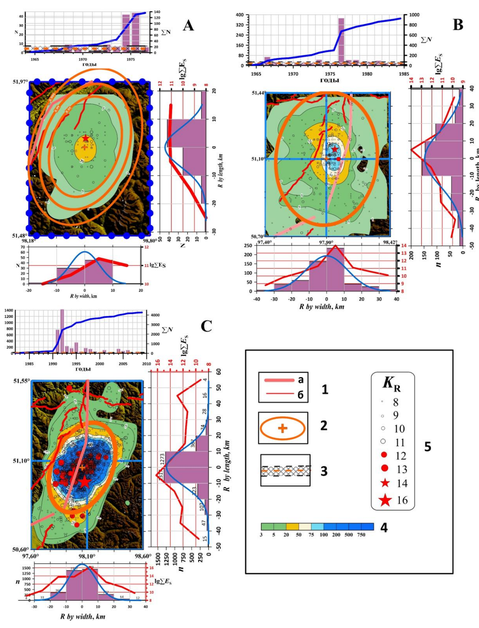


Fig. 2. Spatio-temporal and energy characteristics of seismicity in rectangular sites of aftershocks of 1974 (A), 1976 (B) and 1991 (C)

1 – faults (a – main, b – additional), 2 – ellipses of shock dispersion at the level of 95%, 99%, 99.9% (the center of the ellipse is shown by the marker +), 3 – average annual seismic background with standard deviation, 4 – scale of isolines of epicenter density in 10×10 km2 areas, 5 – earthquake epicenters

In aftershock sequences following a strong (main) earthquake, seismicity is activated with a sharp increase in the rate of aftershock flow and a subsequent decrease in their numbers according to a power law, empirically described by the Omori-Utsu law. Over time, the intensity of aftershocks decreases, and the attenuation formula from the beginning of the power-law decline to the end of the aftershock series has the form of the generalized Omori-Utsu law [Utsu, 2002]

$$N(t) = \frac{K}{(t+c)^p},$$

where $N(t)$ is the number of aftershocks per unit time, t is the time measured from the main shock, $K$, $p$ and $c$ are constants. These parameters were calculated for aftershock sequences.

The parameters c of the Busingol aftershock sequences were determined for the time intervals of maximum correlation of the graphs of changes in the cumulative numbers of aftershocks with the approximating power curve. The maximum correlation of the graphs in the 1976 (correlation coefficient ρ ≈ 0.987) and 1991 (ρ ≈ 0.989) series was detected during the first day after the main shock, and in the 1974 series (ρ ≈ 0.993) – for the entire interval of the aftershock process. The following values of the parameter c were determined: for the 1974 series $c \approx 0.0055$ days (7 min 55 sec), for 1976 $c \approx 0.00377$ days (5 min 26 sec) and for 1991 c≈0.00681 days (9 min 48 sec). The obtained estimates are quite close to the time delay of the first aftershocks after the main earthquakes. In order to detail the studies, the parameters p and K were determined by the cumulative daily samples of aftershock series of 1974, 1976 and 1991 with $K_p \geq 8$ using the least squares method.

The calculation results are presented as variations of the parameter p for the entire duration of the series (fig. 3A) and for 500 days (fig. 3B) for better visualization of rapid changes at the beginning of the series. It is evident that the graphs of the 1974 and 1976 sequences have a similar and rather simple appearance: at the beginning of the series there is a rapid drop from maximum p, then a stage of variations of intermediate values begins, after which a long gradual transition to quasi-linearity and minimum values of p is observed at the end of the series. In general, the changes in the parameter p occur in the same way in all the sequences: three similar stages of different durations are clearly distinguished. The quasi-linear form of the graphs of the parameter K in the 1974 and 1976 sequences, which almost does not change over time, is due to the scale used in fig. 4 A, B: when the scale is increased (to the value of K = 60 (fig. 4C)) at the beginning of the series, a rapid decrease in K is clearly visible, followed by an intermediate stage of gradual decrease, after which the graphs have a quasi-linear form. In the 1974 series, K quickly decreases from 8.9 to 5.8 in the first 15 days, the intermediate stage of decrease ends on the 56th day ($K$ = 3.8), and then a slow decrease to $K$ = 2.7 follows. In the 1976 series, three stages are also distinguished: a fast one at the beginning of the series, when $K$ decreases from 53.2 to 20.5 over the first 22 days, an intermediate one with some fluctuations (on the 64th day $K$=13.3), and a final slow one with $K$=6.7 at the end of the series. The episode of fluctuations in the range p≈1.15±0.06, observed in fig. 5 during the first 170 days of the 1991 aftershock series, is characterized by an increase in $K$ from 332 to 500 in fig. 3 A, B. This is followed by an accelerated decrease, which ends on the 340th day (K=61.7), and a long stage in the form of an oscillatory decrease begins (up to 1400 days, K=25.4). In the final part, the graph has a quasi-linear form and ends at $K$=11.8. Dynamics of the $K$ parameter in fig. 3 corresponds with the behavior of the parameter p in fig. 2, and the changes in the parameters p and $K$ of the aftershock series of 1974, 1976 and 1991 have a consistent, regular character. The revealed differences in the dynamics of the parameters in the initial part of the 1974–1976 and 1991 series are most likely due to a significant difference in the magnitudes of the main shocks and the energy structure of the aftershock series caused by these differences (a small number of moderate and no strong aftershocks in the 1974 and 1976 series and a large number of moderate and fairly strong aftershocks with $K_p \geq 13$ at the beginning of the 1991 series, which, in addition to the dominant effect of the main earthquake, significantly “feed” the energy of seismotectonic deformation at the beginning of the sequence and thereby introduce significant changes in the dynamics of the 1991 aftershock process at the first rapid stage).

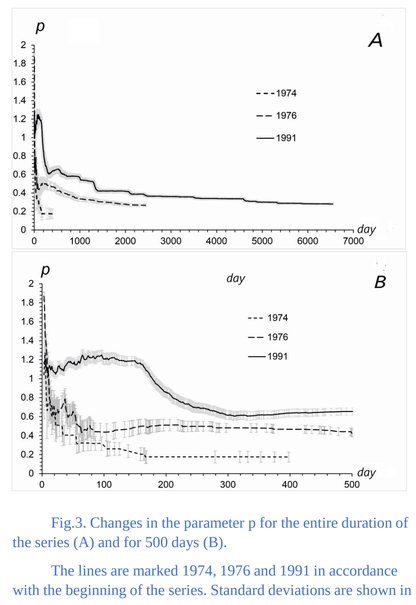


Fig.3. Changes in the parameter p for the entire duration of the series (A) and for 500 days (B).

The lines are marked 1974, 1976 and 1991 in accordance with the beginning of the series. Standard deviations are shown in

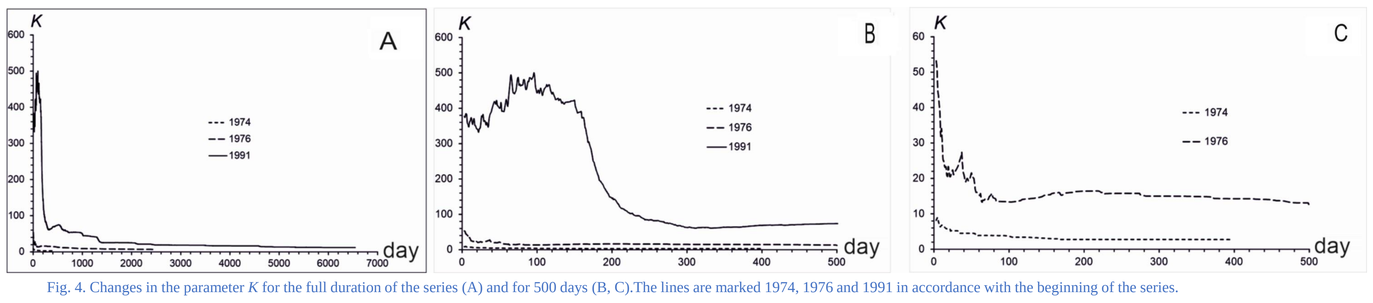


Fig. 4. Changes in the parameter $K$ for the full duration of the series (A) and for 500 days (B, C).The lines are marked 1974, 1976 and 1991 in accordance with the beginning of the series.

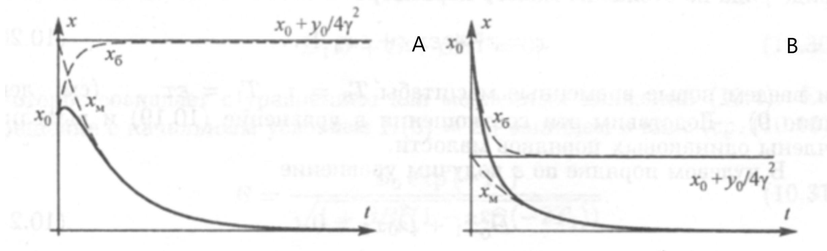


Fig. 5. Dependences x(t) for the Duffing oscillator with strong damping at $y_0 > 0$ (A) and $y_0 < 0$ (B). The dashed lines show the dependences obtained separately for the “fast, $x_b$” and “slow, $x_m$” solutions [from Kuznetsov et al., 2005].

## Conclusions

The procedure for identifying the aftershocks of the Busiingol earthquakes is performed uniformly, in detail and quite correctly: from the epicentral seismicity field of the southwestern flank of the BRS to the sites of aftershock dispersion ellipses taking into account the average flow velocity of background seismicity and groups of weak swarms. The detail and correctness of determining the main parameters are justified by the application of statistical methods to a sufficiently large number of aftershocks in the full range of representative energy classes and an assessment of their reliability.

Based on the results of spatial identification of aftershock sequences of the Busiingol earthquakes of 1974, 1976 and 1991, it was established that the distribution of aftershock epicenters is dominated by common patterns: grouping of shocks in the vicinity of the main earthquake, the epicenter of which is located in the densest part of the cloud and in the center of the aftershock site; oval isometric shape of the epicentral field of aftershocks with increasing concentration towards the epicenter of the main earthquake; elongation of the ellipses of shock dispersion along the BB fault zone; close location of the center of mass of aftershocks and the main event. Nevertheless, there are individual features and differences: the presence of foreshocks in the 1974 series and their absence in the 1976 and 1991 sequences; a significant displacement of the main shock and the epicentral field of aftershocks in 1974 from the BB fault line, whereas in the 1976 and 1991 series these events are close to the fault line; a significant difference in the number of aftershocks in 1974 (78 shocks with $K_p \geq 8$) and 1976 (454 shocks with $K_p \geq 8$) during main earthquakes of the same energy.